Analysis of the Utility of Dynamical Mass Estimators as Applied to Sgr A*

R. F. Trainor[1], A. M. Ghez[2,3]

rtrainor at uci.edu

ABSTRACT

Recent studies of the black hole at the Galactic Center have suggested a mass of 4.36±0.07 million solar masses based on the orbit of S0-2; these estimates are nearly a factor of two greater than estimates based on velocity dispersions a decade ago. This study is the first to use new proper-motion measurements of the central 9" for the explicit purpose of identifying the sources of this discrepancy. We seek to thereby establish bounds on the validity of velocity dispersion based dynamical mass estimators in estimating black hole masses. We base our estimations on 12 years of diffraction limited data from the W. M. Keck 10 m telescopes, including 2 years of data taken using Laser Guide Star Adaptive Optics. Based on the examination of 601 stars, we find that choice of population sample can strongly influence the predictions of dynamical mass estimators. Furthermore, we find evidence supporting the existence of a hole in the distribution of old stars in the region surrounding Sgr A*. We conclude that selection and projection effects easily give rise to a biased sample of stars and that these effects impaired early estimates of the black hole mass. We suggest that a robust understanding of stellar structure is thus essential for confident analyses using dynamical mass estimators, and that caution should be advised in applying these estimators to extra-galactic black hole candidates.

Subject headings: black hole physics – Galaxy:center – infrared:stars – techniques:high angular resolution

1. Introduction

The formation of supermassive black holes (SMBHs) is a poorly understood phenomenon, but one that may be tied to galaxy formation and the development of large-scale structure in the universe. The observations (e.g. Magorrian et al. 1998; Ferrarese & Merritt 2000) of an apparent correlation between the masses of galactic bulges and the central black holes they harbor has only reinforced the possibility of this connection, making the accurate determination of SMBH masses an important tool in studies of galactic structure and formation. Over the last twenty years or so, increasingly compelling evidence has suggested

[1]UCI Department of Physics, Irvine, CA 92697

[2]UCLA Department of Physics and Astronomy, Los Angeles, CA 90095-1562

[3]UCLA Institute of Geophysics and Planetary Physics, Los Angeles, CA 90095-1565

that the radio source Sgr A* at the center of our galaxy is coincident with a SMBH. Many studies in the last decade (e.g Ghez et al. 1998, 2000; Genzel et al. 1996, 2000) have aimed to constrain the mass of this black hole, and from 1996 until the present day the estimated mass has varied greatly. Early estimates of the mass ($2.6 \pm 0.2 \times 10^6$ $M_\odot$ by Ghez et al. 1998) made use of projected mass estimators, such as the well-known virial estimator, by reconstructing the 2D proper motion velocities of stars well within the central parsec. In the last few years, longer baselines have allowed the computation of accelerations for stars near Sgr A*, and coupled with line-of-sight velocities these measurements have allowed the reconstruction of 3D orbits for many stars in the central few arcseconds (see Ghez et al. 2003, 2005; Schödel et al. 2003, Ghez et al., in preparation). These orbits have provided much stronger constraints on the central dark mass and have all but eliminated models of the Galactic Center that do not include a SMBH. More significantly for this study, however, these reconstructed orbits suggest a black hole mass of $4.36 \pm 0.07 \times 10^6$ $M_\odot$ (Ghez et al., in preparation; hereafter G2007) almost a factor of 2 higher than those given by the initial projected mass estimates.

It is likely that the orbital result is the more accurate measurement for a number of reasons. As described in the papers named above, orbital reconstruction gives independent constraints on the black hole mass via well-understood Keplerian physics for every star in the sample, and does not rely on assumptions about the distribution of the stellar population as a whole. As such, the orbital measurements are intrinsically more reliable than those that depend on assumptions about the stellar population as do the projected mass estimates. Furthermore, the larger mass from the orbital reconstruction agrees well with the correlation between bulge and black hole masses (the M-sigma relation) observed in other galaxies, whereas the projected mass estimates deviate more significantly. Therefore it is likely that the projected mass estimates require a re-examination.

This study seeks to identify the source of the discrepancy between these mass estimates through a careful examination of the assumptions inherent in the projected mass estimators, and by conducting our own projected mass estimator analysis on a wider, deeper sample of the stellar population at the galactic center. We also seek to determine the conditions under which these projected mass estimators can be utilized with confidence, and to examine the strengths and pitfalls of some of the more commonly used mass estimators. We hypothesize that the initial mass estimates were marred by one or more of the following factors: large measurement errors in the utilized data sets, a population of stars at the galactic center that violates the assumptions of the projected mass estimators, and/or a sample of stars that was biased through selection effects, and thus unrepresentative of the true stellar population.

2. Observations & Data Analysis

New measurements of proper-motion velocities were reconstructed from K-band (λ=2.2 μm) images of the galaxy's central stellar cluster using the NIRC (Matthews & Soifer 1994; Matthews et al. 1996) and NIRC2 (K. Matthews, in preparation) near-infrared cameras on the Keck II telescope. This study uses 34 epochs of diffraction-limited images taken initially using speckle imaging but including 7 epochs of laser

guide star adaptive optics (LGS AO, see van Dam et al. 2006; Wizinowich et al. 2006) images obtained with NIRC2. The imaging techniques and data sets are described in detail in G2007, and all but the most recent (LGS AO) data are described in earlier papers (Ghez et al. 1998, 2000; Lu et al. 2005; Rafelski et al. 2007).

Data analysis was performed using the Python interactive programming language, with extensive use of the 'numarray' and 'pylab' modules. Where appropriate, data fitting was performed using the 'mpfit' module.

All calculations of distances and velocities in the galactic center region were made assuming a distance to the galactic center (R_0) of 8 kpc, in keeping with the majority of the literature. As proper-motion mass estimates of the central black hole are proportional to the cube of R_0, mass estimates from the literature have been renormalized to reflect this choice of distance when used for direct comparison.

2.1. Projected mass estimators

This study used the Bahcall-Tremaine (BT) and Virial mass estimators described in Ghez et al. (1998) (hereafter G98) in order to directly compare the results of these mass estimators on new data with their results on the 1998 data. As in G98, we define the Virial and BT estimators, respectively, by the following:

$$M_{vir} = \frac{3\pi}{2G} \frac{< v^2 >}{< 1/R >} \tag{1}$$

$$M_{BT} = \frac{16}{\pi G} < v^2 R > \tag{2}$$

The assumptions and conditions of these mass estimators are described in that paper, and in Bahcall & Tremaine (1981) in greater detail. As the 2D velocities of the stars in the sample are now quite well resolved, a more powerful mass estimator was used to eliminate dependence upon the radial or tangential distribution of the stellar orbits. This estimator is a variant on the projected mass estimator developed in Leonard & Merritt (1989) for use with open stellar clusters.

Their derivation from Jean's equations for a spherically-symmetric stellar cluster holds just as well for a cluster of stars around a SMBH until the imposition of a choice of mass distribution $M(r)$ (see their Eq. 19). In the case of a region with a mass distribution dominated by a central black hole, $M(r)$ just becomes M for the entire range of r where the black hole mass can be considered to dominate, and the estimator can be written as

$$M = \frac{16}{3\pi G} < (2v_R^2 + v_T^2)R > \tag{3}$$

which is just a factor of 2 smaller than the equivalent estimator for an open cluster. As the central black hole dominates the mass distribution out to $\sim$1 pc, we have adopted this for our purposes and refer to the above formula henceforth as the Leonard-Merritt (LM) mass estimator.

2.2. Samples of stellar population

In total, 1660 stars were included in the data set, but cuts were applied to ensure the elimination of non-physical sources. We conservatively imposed the constraint of appearance in at least 6 of the 7 LGS AO epochs in order to be considered a physical source; this left 601 stars in our sample. This sample was then divided into four overlapping sub-samples in order to investigate the effect of population sample on the mass estimates. The first, known as 'all', included all 601 stars that met the LGS AO constraints. The second, 'yngstars', included 43 stars previously known to have ages of 2-7 Myr (see Paumard et al. 2006; Lu et al. 2006) that also meet the LGS AO cut. The identification of this sub-sample is significant because many of these stars have been shown (see e.g. Levin & Beloborodov 2003; Genzel et al. 2003; Lu et al. 2006) to lie in a disc, thus violating the isotropy assumption of the projected mass estimators. The third sub-sample, 'oldstars', consisted of the 558 stars in 'all' that do not belong to the population of known young stars. In order to compare results from the same sample of stars used in earlier studies, 87 of the 90 stars included in G98[1] were considered as a fourth sub-sample called '98stars', with the 3 omitted stars being eliminated because they failed the requirement of inclusion in 6 of the 7 LGS AO epochs.[2] This study also uses position and velocity data from the literature (G98) to compare the effect of measurement error/uncertainties on that study and on the new measurements.

2.3. Bias removal

Because measurement uncertainties tend to spread out the distribution of measured values, and the velocity dispersion is a measure of the intrinsic spread of velocity values, velocity measurement errors create a bias toward larger calculated dispersions. In order to account for and remove this bias, we have defined the intrinsic velocity dispersion $\sigma_{int}^2 = \sigma_{meas}^2 - \delta_v^2$, where $\delta_v^2 = \Sigma_{i=1}^{N}(\delta_{vx,i}^2 + \delta_{vy,i}^2)/(2(N-1))$ is the bias term. All reported values of the velocity dispersion will refer to σ_{int}. It should be noted that the quoted results from G98 and other papers have already been subjected to this process by the authors.

2.4. Analysis of Anisotropy

Anisotropy in the 2D distribution of velocity dispersions was used as a probe for anisotropy in the stellar orbits and structure. The 2D distribution of the velocity dispersions was determined by dividing the central 10" into 0.″25x0.″25 bins. The velocity dispersion for each bin was defined to be the dispersion of all stars within 0.″75 of the north-east corner of the bin. As the population sample showed a marked non-physical decrease in number density at projected distances more than 4.″5-5" from Sgr A*, only bins within

[1]Several stars in G98 are now known by different names, and as such appear under their new names in the new data sets

[2]IRS 29N was detected in 5 LGS AO epochs; S0-8 and S3-12 were detected in 3 LGS AO epochs

4.″5 of Sgr A* were included in the final analysis.[3]

Because the velocity dispersions are expected to fall off as a function of distance from the central black hole, checks for anisotropy compared the velocity dispersion of each bin to those of bins a similar projected distance from Sgr A*. The sample was divided into six 0.″75 radial annuli, as shown in Fig. 1. For each bin, the deviation in the velocity dispersion of the bin from the velocity dispersion of its entire radial annulus was calculated; this deviation was then divided by the error in the dispersion[4] for that bin in order to calculate the significance of the deviation.

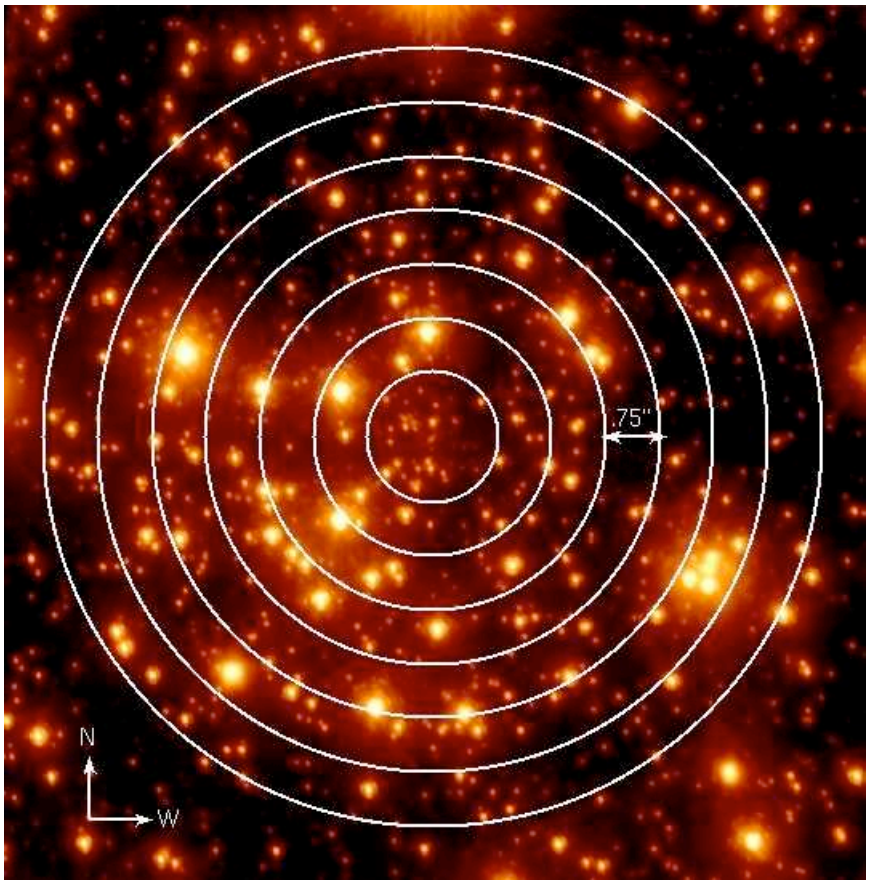

Fig. 1.— Annuli used to group bins of stars, plotted over image of the central 10". Annuli have widths of 0.″75 and are centered on Sgr A*.

[3]The analysis thus included some stars more than 4.″5 in projected distance from Sgr A*, as bins at a projected distance of 4.″5 included stars an additional 0.″75 away.

[4]The error in the velocity dispersion is given by $\delta_{\sigma_v} = \sigma_v/(2(N_{bin}-1))$, where N_{bin} is the number of stars in that bin

3. Results

3.1. Effect of measurement error

Computation of the intrinsic velocity dispersion and bias term for the velocity measurements reported in G98 yielded $\sigma_v = 229$ km/s with a bias $\delta_v = 144$ km/s; this represents a fractional bias $\delta_v^2/\sigma_v^2 = 0.395$. For the new dataset, the fractional bias in the velocity dispersion for the '98stars' sample was $\delta_v^2/\sigma_v^2 = 2.14 \times 10^{-4}$. A comparison of the estimated SMBH mass between the G98 results and new measurements using the same mass estimators, as well as the LM estimator, is presented in Table 1.

SMBH Mass Estimates (10^6 $M_\odot$) from '98stars' sample

G98	Virial	BT	LM
2.6 ± 0.2	2.57 ± 0.61	3.00 ± 0.34	2.77 ± 0.31

Table 1: Comparison of mass estimates for the central black hole between reported results in Ghez et al. (1998) and new results using same set of stars. Reported errors represent 1σ.

3.2. Violations of estimator assumptions in central cluster

3.2.1. Anisotropy in the central cluster

After computing the deviations in the velocity dispersion from the overall annular values as described in §2.4, the significances of the deviations were plotted in 2D (Fig. 2, left). Of the 958 included bins, 953 were consistent with the annular dispersion to within 3σ. The remaining 5 bins all had dispersions lower than their relevant annular values. When the deviations of the bins were plotted as a histogram together (Fig. 2, right), they displayed a fairly Gaussian distribution with mean $\sim$0 and standard deviation $\sim$1, though with evidence for a tail on the negative side.

3.2.2. Orbital dependence of mass estimate

The results of applying the Virial, BT and LM estimators to the '98stars' sample have already been presented in Table 1. The application of these estimators to the 'yngstars', 'oldstars' and 'all' samples are presented in Table 2. The BT and LM estimates for the 'oldstars' and 'all' samples are consistent with the orbital result of 4.36×10^6 $M_\odot$ within 1σ; the substantially lower estimates from the 'yngstars' sample and the Virial estimator are explored in §4.3 and §4.4.

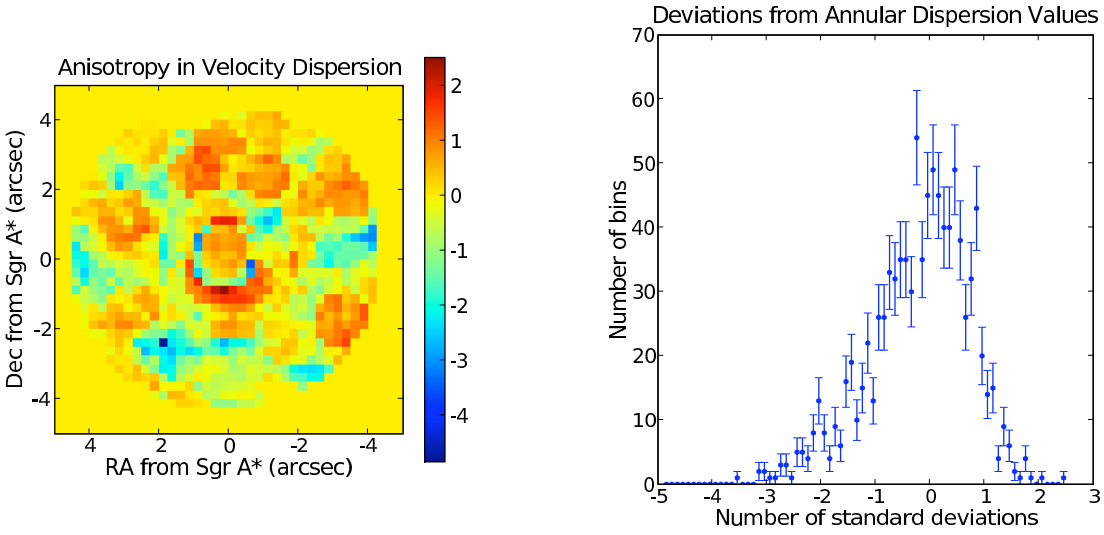

Fig. 2.— LEFT: Significance of the deviation of the velocity dispersion of stars in each bin compared to the velocity dispersion of stars in the entire 0.″75 radial annulus. Color denotes deviation in units of sigma. RIGHT: Deviations of all bins included in plot on left, plotted as histogram and displaying fairly Gaussian distribution with mean ~ 0 and $\sigma_v \sim 1$.

3.3. Effect of population sample on mass estimate

Tables 1 and 2 display the mass estimates derived from the four sub-samples of the stellar population. The 'oldstars' and 'all' estimates were within 1σ of each other for all three estimators; however, the differences among the 'oldstars'/'all' sets, the 'yngstars' set and the '98stars' set were much more significant. Note that, with the exception of the Virial estimates, the 'oldstars' and 'all' estimators yield results consistent with the mass estimate of 4.36 ± 0.07 million solar masses given by G2007, and differ with high significance from the G98 results.

An additional check on the effect of population sample was performed by making mass estimates based on dividing the population samples into radial annuli. The 'oldstars' and 'yngstars' samples were divided into 0.″75 annular bins, and the mass estimates are plotted vs. bin radius in Fig. 3. The 'oldstars' sample displays a clear increase in estimated enclosed mass with increasing radius; the 'yngstars' sample, while not constant with radius, does not display this relationship. The significance of these effects will be discussed in §4.

SMBH Mass Estimates (10^6 $M_\odot$)

Sample	Virial	BT	LM
'yngstars'	3.86 ± 1.36	3.67 ± 0.45	3.40 ± 0.42
'oldstars'	3.07 ± 0.18	4.45 ± 0.24	4.24 ± 0.25
'all'	3.21 ± 0.29	4.39 ± 0.23	4.18 ± 0.24

Table 2: Comparison of mass estimates for the central black hole between three mass estimators for each of three different population samples described in §2.2. Reported errors represent 1 σ.

4. Discussion

4.1. Significance of measurement error

From Table 1 it is clear that the use of newer data on the same set of stars as G98 produces no significant change in the mass estimate; all three mass estimators are consistent within errors with the G98 results. This insensitivity to velocity errors in the mass estimate is due to the bias removal process described in §2.3, but accounting for errors in this manner can only be performed accurately if the measurement errors are well-understood and correctly quantified. Thus consistency between the G98 results and the new results on the '98stars' data sample suggests that the errors were indeed quantified accurately in 1998, rather than there being an overestimate in the error, which could have led to the underestimate in the mass by allowing too large a bias term to be subtracted off. For our study, however, this merely means that measurement errors have not contributed significantly to the discrepancy in the mass estimates.

4.2. Validity of mass estimator assumptions

The velocity dispersions in the 'all' sample were used to determine the anisotropy inherent in the stellar population. As described in §3.2.1, the variations in the 2D distribution of the velocity dispersions in the central 9" are consistent with random variation, as very few bins differ from their expected values by more than 3σ and variations take on a fairly Gaussian profile. Thus the stellar proper-motion velocities are reasonably isotropic. Furthermore, as it is unlikely that we are observing the galactic center from any special vantage point, we can infer that the observed isotropy in the plane of our sky is the consequence of isotropy in the 3D distribution of the stellar positions and velocities.

The results of §3.2.2 and Tables 1 and 2 demonstrate that the early mass estimates made appropriate assumptions regarding the eccentricities of the stellar orbits. Recall that the BT mass estimator differs by a factor of 2 depending on whether the orbits are radial or isotropic. As the LM estimator is not affected by this distinction, the agreement of the BT and LM estimates for all three sub-samples validates the isotropic orbits assumed in G98 and other early estimations. The low mass estimates given by the Virial estimator for the 'oldstars' and 'all' samples are most likely due to a hole in the distribution of old stars, the evidence and significance of which is described below in §4.4. The lack of significant anisotropy in the velocity dispersion

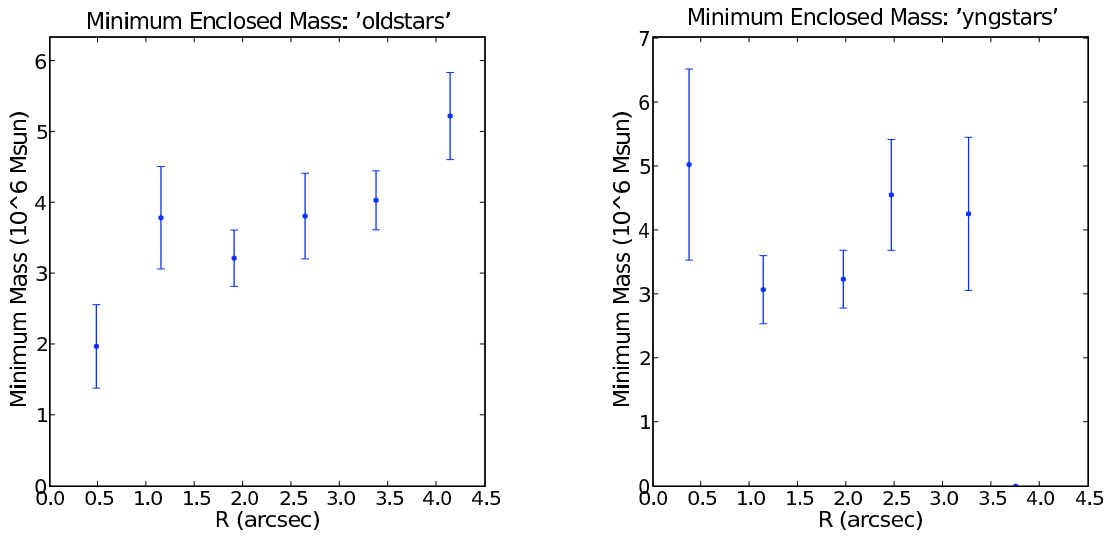

Fig. 3.— Enclosed mass estimates for stars divided into 0.″75 radial annuli, separately plotted for the 'oldstars' and 'yngstars' population samples. All plotted estimates were made using the LM estimator. The 'yngstars' plot has no data for $R > 3.''5$ as there were too few stars with sufficiently large projected radaii in that sample.

profile suggests that the stellar system is consistent with the assumptions of spherical symmetry intrinsic to the projected mass estimators. Similarly, the agreement between the LM and BT mass estimates suggests that the assumptions regarding orbital structure were likewise satisfied in G98 and other early papers. The main remaining assumption of the estimators concerns the variation of the stellar density as a function of radius. As we lack direct information about the LOS position of stars relative to Sgr A*, it is very difficult to test for anomalies in the stellar distribution–such as a hole–directly. Again, we present the evidence of such a hole in §4.4, and here merely affirm that the discrepancy in the mass estimates was not due to violations of the estimator assumptions regarding isotropy and orbital structure.

4.3. Population Effects

The close correspondence of the mass estimates based on the 'all' and 'oldstars' sub-samples is due to the fact that the vast majority of the stars in the population are non-young stars, and thus the 'all' sub-sample is dominated by the same stars that make up the 'oldstars' sub-sample. The discrepancies when using the 'yngstars' sample likely arise from the fact that much of the young star population at the galactic center is known to reside in one or more disks (Levin & Beloborodov 2003; Genzel et al. 2003; Lu et al. 2006). As the young stars do not constitute a relaxed, isotropic population, the projected mass estimators do not yield accurate results when applied to this population. Therefore it is the difference between the 'all'/'old'

and ‘98stars’ population samples that constitutes the significant result. As noted above, the ‘98stars’ results are consistent with the mass estimates of G98; the ‘all’ and ‘oldstars’ results are consistent with G2007 and the estimates made by orbital reconstruction. However, we have now observed this discrepancy in a case where the only difference is in the choice of population sample, as the mass estimation technique is the same. Thus we can speculate on how these samples might generate different estimates based on some of their other characteristics, rather than the estimation methods. As the differences between the ‘all’ and ‘oldstars’ samples are negligible, we compare only the ‘all’ and ‘98stars’ sample.

The ‘98stars’ sample is completely contained within the ‘all’ sample but clearly is not representative of the ‘all’ sample as a whole. The reasons for this stem from the technical constraints in place when the G98 data was being collected. Without the benefits of AO, source confusion and background inhibited the identification of faint sources, and so the ‘all’ sample represents a much deeper scan of the central few arcseconds. In the ‘98stars’ sample only 11 of 87 stars have magnitude 15 or higher, whereas in the ‘all’ sample 415 of the 601 stars are of at least that magnitude. As image correction with AO is also faster than speckle imaging, AO scans imaged a larger area of the galactic center, and thus the ‘all’ sample represents a wider field of view as well. The ‘98stars’ sample had a mean projected distance (R) from Sgr A* of $2\farcs014$ and only 8 stars with $R > 3\farcs5$, while the ‘all’ sample had a mean R of $3\farcs139$ and 246 stars with $R > 3\farcs5$. In this manner, the data collected with AO eliminated the artificial brightness cut inherent in the G98 collection methods and enabled the creation of the wider, deeper ‘all’ sample, which is presumably more characteristic of the true stellar population. Recalling from §1 that the mass estimates based on orbital reconstruction are preferred based on the precision of the technique and the agreement with the M-sigma relation observed in other galaxies, it is heartening that we arrive at these same estimates from the ostensibly more representative population sample.

4.4. Evidence for a hole in stellar distribution

Although we are able to recover the orbital-reconstruction results by use of a larger, more representative population sample, it is worth investigating the physical reasons by which the original set of stars underestimated the SMBH mass. Previous studies (see Figer et al. 2003, and references therein) have presented evidence for a hole in the old-star distribution at the galactic center, that is, an uncharacteristically low number of old stars in the immediate region around Sgr A*. Though the results of Figer et al. (2003) suggest a hole characterized by a radius of $\sim$0.4 pc,[5] a hole of smaller radius could give rise to many of the anomalous results of our data analysis. We here present qualitatively how such a hole could produce the increase in reconstructed mass with radius displayed in Fig. 3, which would then create the bias toward low-mass results in the G98 mass estimates and the new Virial mass estimates.

Because of the lack of information on the LOS displacement of stars relative to Sgr A*, the 2D projected mass estimators must assume that stars with small projected displacements (R) generally have small 3D

[5] 10” with R_0 =8 kpc

displacements as well. However, if there are few stars that actually lie near Sgr A* in 3D space, stars with small R will in fact have large LOS displacements. From Keplerian dynamics, stars close to the black hole should in general move more quickly than stars farther away, but as the stars with small projected displacements are not actually close to the black hole, they display velocities too low for a given central mass at their assumed orbital distances. Thus the low velocities coupled with small values of R cause an underestimate of the black hole mass at small projected radii. This effect is most pronounced at the smallest values of R and lessens as R increases; hence the increase in reconstructed masses with increasing R displayed in Fig. 3.

This bias toward a small reconstructed mass for the stars at small projected radii also leads to the underestimates in G98 and by the Virial mass estimator. As discussed above, the stellar sample used in G98 was dominated by stars with small projected displacements from Sgr A*, and therefore the mass results were biased toward small values. The new analysis, using the 'oldstars'/'all' samples, contained enough stars with larger values of R ($> 3\farcs5$) that the hole did not dominate the stellar distribution, suggesting that there is a hole characterized by a radius of $\sim 3\farcs5$, or $\sim$.14 pc assuming a value of 8 kpc for R_0.

The error in the Virial estimates stems from a bias in the Virial mass estimator toward stars with small projected radii and high velocities. This bias is discussed in some detail in Bahcall & Tremaine (1981), but it is not difficult to see from the form of the Virial estimator (Eq. 1); stars with small projected radii provide the principal contribution to $< 1/R >$, and, as these stars tend to be moving faster than those at large radii, they also tend to dominate $< v^2 >$. In this manner the sample of stars at small projected radii plays the dominant role in determining the Virial mass estimate, and thus biases the estimate toward smaller values.

5. Conclusions

We have here presented evidence that the early dynamical mass estimates of the central SMBH, such as the results of G98, were biased by projection effects in their population samples. We have demonstrated that these dynamical mass estimators do in fact corroborate the mass estimates based on orbital reconstruction and the observed M-sigma relation when applied to a wider, deeper sample of the stellar population at the galactic center. Finally, we present an explanation of the bias toward small masses in terms of a hole in the population of old stars at the galactic center. A further exploration of the quantitative effects of such a hole through Monte Carlo simulations would go far in confirming its existence and extent.

As displayed by the consistent early underestimates of the black hole mass, a thorough understanding of central structure is essential in order to obtain accurate estimates of SMBH masses in other galaxies. This is especially true because the vast distances to even the nearest extra-galactic SMBHs will likely limit future studies through the same selection effects that impaired the early studies of our galactic center. Understanding the nature and formation mechanisms of the structure in our own galactic center could allow the extension of dynamical mass estimation techniques, with accurate assumptions, to SMBHs in other galaxies. Until such a general understanding is reached, however, we recommend applying the dynamical mass estimators only to very complete population samples and structures with well-known geometries.

6. Acknowledgements

RT would like thank UCLA and the NSF for support via the Research Experience for Undergraduates program. Thanks also to the administrative aid of Françoise Quéval, to Brad Hansen for help on dynamics, and very special thanks to AMG as well as S. Yelda and J. Lu for their willingness to help with even the most trifling problems throughout the research process.

REFERENCES

Bahcall, J. N. & Tremaine, S. 1981, ApJ, 244, 805

Ferrarese, L. & Merritt, D. 2000, ApJ, 539, L9

Figer, D. F., Gilmore, D., Kim, S. S., Morris, M., Becklin, E. E., McLean, I. S., Gilbert, A. M., Graham, J. R., Larkin, J. E., Levenson, N. A., & Teplitz, H. I. 2003, ApJ, 599, 1139

Genzel, R., Pichon, C., Eckart, A., Gerhard, O. E., & Ott, T. 2000, MNRAS, 317, 348

Genzel, R., Schödel, R., Ott, T., Eisenhauer, F., Hofmann, R., Lehnert, M., Eckart, A., Alexander, T., Sternberg, A., Lenzen, R., Clénet, Y., Lacombe, F., Rouan, D., Renzini, A., & Tacconi-Garman, L. E. 2003, ApJ, 594, 812

Genzel, R., Thatte, N., Krabbe, A., Kroker, H., & Tacconi-Garman, L. E. 1996, ApJ, 472, 153

Ghez, A. M., Duchêne, G., Matthews, K., Hornstein, S. D., Tanner, A., Larkin, J., Morris, M., Becklin, E. E., Salim, S., Kremenek, T., Thompson, D., Soifer, B. T., Neugebauer, G., & McLean, I. 2003, ApJ, 586, L127

Ghez, A. M., Klein, B. L., Morris, M., & Becklin, E. E. 1998, ApJ, 509, 678

Ghez, A. M., Morris, M., Becklin, E. E., Tanner, A., & Kremenek, T. 2000, Nature, 407, 349

Ghez, A. M., Salim, S., Hornstein, S. D., Tanner, A., Lu, J. R., Morris, M., Becklin, E. E., & Duchêne, G. 2005, ApJ, 620, 744

Leonard, P. J. T. & Merritt, D. 1989, ApJ, 339, 195

Levin, Y. & Beloborodov, A. M. 2003, ApJ, 590, L33

Lu, J. R., Ghez, A. M., Hornstein, S. D., Morris, M., & Becklin, E. E. 2005, ApJ, 625, L51

Lu, J. R., Ghez, A. M., Hornstein, S. D., Morris, M., Matthews, K., Thompson, D. J., & Becklin, E. E. 2006, in Conf. Proceed.: "From the Center of the Milky Way to Nearby Low-Luminosity Galactic Nuclei", ed. R. Schödel, G. C. Bower, M. P. Muno, S. Nayakshin, & T. Ott

Magorrian, J., Tremaine, S., Richstone, D., Bender, R., Bower, G., Dressler, A., Faber, S. M., Gebhardt, K., Green, R., Grillmair, C., Kormendy, J., & Lauer, T. 1998, AJ, 115, 2285

Matthews, K., Ghez, A. M., Weinberger, A. J., & Neugebauer, G. 1996, PASP, 108, 615

Matthews, K. & Soifer, B. T. 1994, Experimental Astronomy, 3, 77

Paumard, T., Genzel, R., Martins, F., Nayakshin, S., Beloborodov, A. M., Levin, Y., Trippe, S., Eisenhauer, F., Ott, T., Gillessen, S., Abuter, R., Cuadra, J., Alexander, T., & Sternberg, A. 2006, ApJ, 643, 1011

Rafelski, M., Ghez, A. M., Hornstein, S. D., Lu, J. R., & Morris, M. 2007, ApJ, 659, 1241

Schödel, R., Ott, T., Genzel, R., Eckart, A., Mouawad, N., & Alexander, T. 2003, ApJ, 596, 1015

van Dam, M. A., Bouchez, A. H., Le Mignant, D., Johansson, E. M., Wizinowich, P. L., Campbell, R. D., Chin, J. C. Y., Hartman, S. K., Lafon, R. E., Stomski, Jr., P. J., & Summers, D. M. 2006, PASP, 118, 310

Wizinowich, P. L., Le Mignant, D., Bouchez, A. H., Campbell, R. D., Chin, J. C. Y., Contos, A. R., van Dam, M. A., Hartman, S. K., Johansson, E. M., Lafon, R. E., Lewis, H., Stomski, P. J., Summers, D. M., Brown, C. G., Danforth, P. M., Max, C. E., & Pennington, D. M. 2006, PASP, 118, 297